Hindawi Publishing Corporation
International Journal of Distributed Sensor Networks
Volume 2013, Article ID 256569, 16 pages
http://dx.doi.org/10.1155/2013/256569

Research Article

eLighthouse: Enhance Solar Power Coverage in Renewable Sensor Networks

Peng Liu,[1] Yifan Wu,[1] Jian Qiu,[1] Guojun Dai,[1] and Tingting Fu[2]

[1] *Institute of Computer Application Technology, Hangzhou Dianzi University, Hangzhou 310018, China*
[2] *Institute of Graphics and Image, Hangzhou Dianzi University, Hangzhou 310018, China*

Correspondence should be addressed to Tingting Fu; ftt@hdu.edu.cn

Received 16 May 2013; Revised 15 August 2013; Accepted 7 September 2013

Academic Editor: Aravind Kailas

Energy harvesting from ambient resource such as solar power improves the sustainability and continuous monitoring capability of sensor nodes. However, energy conservation and harvesting can hardly provide a complete solution due to two main reasons: the energy harvesting capabilities/opportunities are seriously affected by spatial and temporal facts regarding the location of sensor deployment, and distributed processing of sensing and communication are also uneven throughout the network which leads to unbalanced energy consumption. In this paper, we propose an energy transfer system called eLighthouse to level the energy harvesting and consumption of solar-powered WSN. An energy-hub equipment has been brought forward utilizing a controlled retroreflector to forward sunlight to the appropriate nodes which urgently require recharging. The scheduling algorithm among multiple nodes is also included in this paper which helps to maintain the maximum number of nodes in active state; the localization algorithm which enables the controlled retroreflector for pointing correctly is also a key contribution of this paper. The experimental and simulation results both demonstrated that the proposed system can maximize the utilization of the solar power charging technique effectively to prolong the network lifetime and build up a sustainable WSN.

1. Introduction

Limited energy supply has been the main constraint of battery-powered system such as wireless sensor networks which provide continuous monitoring in ambient environment. It greatly affects the sustainability of WSNs and has disproportionate impact on the fidelity. In this area, the recent research topics are mainly focused on two categories: energy saving and energy harvesting.

A natural mechanism of energy saving is enhancing network protocols, such as energy-efficient MAC protocols, routing protocols, and data aggregation as shown in [1–3]. The goals of these researches are not only to reduce the energy consumption rate but also to balance it. However, these schemes can only prolong the network lifetime to a limited extend but fail to make it sustainable. A promising solution to this problem is to explore energy harvesting and acquiring techniques. Solar power, wind power, and vibration power have all been introduced as perspective energy resource of tiny sensor nodes. Corresponding hardware design and experiments have also been introduced in many papers although it still suffers some limitations such as costliness, inflexibility, and low efficiency. Furthermore, without sufficient energy acquiring approaches, these methods cannot work well.

On one hand, as a network performing distributed monitoring tasks, data communication and collection process are seriously dependent on task requirement and network topology. Sink nodes and other nodes near hot spots or in a busy route tend to consume their energy more rapidly which means energy consumption among the network that is unevenly distributed. On the other hand, the energy harvesting capability at each node may vary significantly due to environmental geometric. For example, the amount of harvested solar power in a sensor node varies due to factors of weather, location, and time, in spite of Maximum Power Point Tracking function being used. In one word, the energy harvesting is unbalanced as well as energy consumption. Researches have been carried out to balance the energy distribution, such as [4, 5]. However, these approaches only

consider the energy usage pattern corresponding to the energy harvesting rate, in which the faster recharged nodes carry more operation responses. It is not always feasible to level data communication by the energy harvesting capability. A heavy loaded sensor node may be deployed at energy-poor locations and become the bottleneck of the entire network.

To balance energy between nodes, energy share system could be a solution. Energy can be transferred to other nodes via wires, microwave, magnetic resonance, laser, and so on. Wired transfer does not fit for wireless sensor networks and Magnetic resonance has very low efficiency. Microwave and Laser require additional high-cost equipments which have huge overhead under current technology. Despite the poor performance of current energy sharing system, the idea of energy transfer between sensor nodes still has its potential in energy balancing. The key design goal is to improve the energy transfer efficiency. In our opinion, transferring the initial state of the harvested energy may be a promising way. Therefore, in this paper, we propose a sunlight reflection based resource energy transfer method for solar energy harvesting sensor networks. During daytime, it does not produce special means of energy such as electrical, laser, magnetic resonance, microwave, and so on but only relay the ambient energy in the initial state. Sunlight is reflected by a retroreflector for recharging capability enhancement to specified nodes in an inappropriate place, for example, nodes in shaded area or with heavy loads. To improve efficiency, spare energy accumulated during daytime can also be transferred to nodes by wireless energy transfer means in the night or during bad weather.

The proposed system consists of (1) a sunlight reflection and solar power harvesting station called energy hub (2) wireless sensor nodes equipped with solar panel and light sensor. The energy hub can adjust the onboard retroreflector and reflect sunlight to enhance the recharging capability of specified nodes and charge them like a lighthouse. Fundamental experiments have been carried out to prove the feasibility of the proposed mechanism as well as evaluation of the energy transfer efficiency. A prototype system has been produced and the corresponding scheduling algorithm has also been introduced to ensure the network lifetime extension, which aims to build up a sustainable sensor network system. However, we meet some design and implementation challenges, such as accurate localization of the solar board with a maximum tolerable error of centimeter level, precise sunlight reflection positioning, and real-time energy recharging scheduling.

This method fits well for infrastructured environment as it requires line-of-sight (between the energy hub and the sensor node with solar panel). As shown in Figure 1, each node may have different opportunities to receive sunlight (denoted by percentage) due to the movement of the sun. By applying the proposed method, it can efficiently provide reflected sunlight or wireless energy against the shadow. For large networks in a more complex environment, our method can also improve energy efficiency by deploying energy hubs locally and carefully.

More specifically, the main contributions of this paper are concluded as follows.

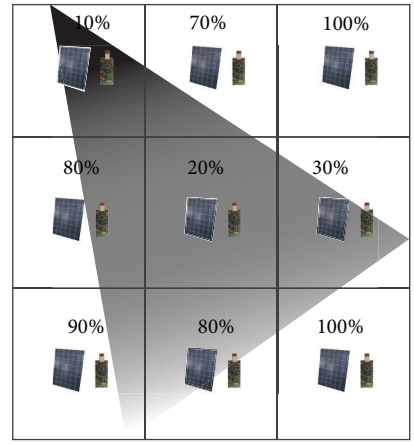

Figure 1: Energy harvesting ability varies from node to node.

(i) We designed and implemented a solar power transfer system for energy harvesting sensor networks, which is a novel means of efficient initial state energy transfer scheme.

(ii) We proposed a sunlight reflection strategy which can reflect sunlight to the solar panel of the nodes in need. The strategy includes solar panel covering and retroreflector adjusting.

(iii) We have proposed an accurate node locating algorithm for sensor node localization, which combines camera and RSSI locating method.

(iv) We have developed a charging scheduling algorithm which guarantees the sustainability of sensor nodes.

(v) We conducted model simulations and also built a proof-of-concept prototype of the system and conducted extensive experiments on the prototype to evaluate its feasibility and performance. The results indicate that our system can efficiently enhance sunlight coverage and improve network performance.

The remainder of the paper is organized as follows. In Section 1, the motivation is introduced, while, in Section 2, related works are described and evaluated. The system model and design are discussed in Section 3, and the node locating mechanism is presented in Section 4. Section 5 discusses the scheduling of the charging sequence, followed by simulation and experimental evaluations in Section 6. Finally, Section 7 concludes the paper.

2. Related Work

To prolong lifetime of sensor networks, energy harvesting has been proved to be a promising key. Solar power, wind power, vibration, and even human power [6] can all be the energy source. Design, modeling, and capacity planning for energy harvesting sensor network are evaluated in [7]. However, the energy harvesting opportunity of each node is far from each other and varies with respect to temporal and spatial facts.

Energy share methods are introduced to solve this bottleneck problem, which implies energy transfer between nodes

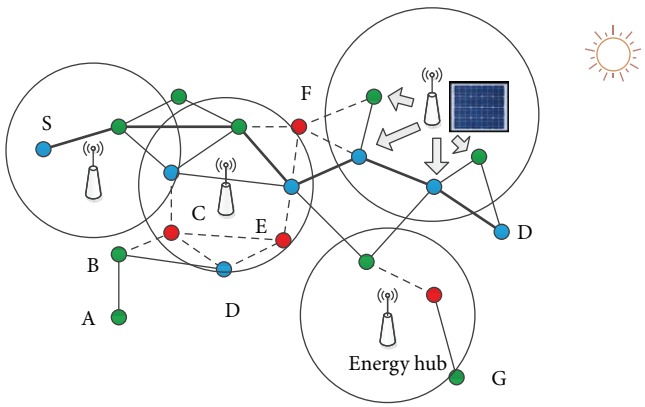

Figure 2: Sensor network architecture with energy hubs.

or from energy station to nodes by means of wired or wireless electrical power exchange technologies. Magnetic resonance, developed by Kurs et al. [8], has become a major technique for wireless energy transfer, based on which some recharging scheduling algorithms have been developed, [9, 10]. Other studies utilizing wired energy transfer are conducted as well. Zhu [11] developed an energy charging and discharging mechanism using an array of ultracapacitors as the main component of an energy router through wired connections, which is known as eShare. However, according to [10], wireless charging efficiency is seriously affected by distance. Charging efficiency is approximately 1.5% when the energy receiver is 10 cm away from the charger. The charging efficiency decreases to zero when the distance approaches 100 cm. The controlled electrical energy transfer between wired ultracapacitors is also not as regular as mentioned in [11] due to physical characteristics of the component, which has some nonlinear features. Another main disadvantage is the low efficiency caused by the wasted energy in transfer circuit. Above all, electrical energy share schemes are still in a design or laboratory experiment level at the recent stage.

Localization has been a hot topic for years. However, the accuracy depends on node density and available facilities. Most of the range-based methods can be concluded into four categories, which are time of arrival (TOA), time difference of arrival (TDOA) [12], angle of arrival (AOA) [13] and received signal strength indicator (RSSI) [14]. Range-free methods are mentioned in [15–17].

References [18, 19], which use Corner Cube Retroreflector (CCR) to transfer man-made laser and mirrors to transfer lamplight by optical means, are the most similar work compared with our approach. In [20], the authors propose using external energy transmitters (ETs) to charging sensor nodes by wireless means. ETs are assumed that they have endless power and can be deployed randomly or predetermined. The paper does not discuss the placement of ETs but proves the feasibility of this energy station-based method and the routing and data transmission issues under the circumstance. References [9, 21–23] both focus on mobile energy station which can prolong network lifetime by traveling among nodes and charging them wirelessly. The main concern is the movement and trajectory of mobile energy station (also be called ferry, charging vehicle, mobile charger, etc.). Watfa et al. [24] try to extend current one-hop wireless energy transfer to a multihop manner. They investigate both theoretically and through simulations whether the physical phenomenon of long-lifetime resonant electromagnetic states with localized slowly evanescent field patterns can be used to transfer energy efficiently over multiple hops. In [25], the placement of RF power transmitters is bounded with missions of sensor nodes. RF power transmitters will be moved to Landmarks among sensor networks according to current missions and maximize the energy usage and the profit. The key problem is how to choose Landmarks and the authors propose ILP to solve it.

3. System Description

3.1. System Overview. As can be seen from Figure 2, in eLighthouse system, there are sensor nodes and energy hubs. Each energy hub can cover certain amount of sensor nodes. The coverage area can be either identical or variant. The energy to power a single sensor node comes from energy harvesting from solar power. Sensor nodes might run out their batteries so that part of communication connections between nodes becomes intermittent shown as dashed lines in the figure. There are two major problems. First, because of the movement of the sun and shadow of the environment, each node does not have an equal opportunity to receive sun radiation. The principle of eLighthouse system is based on sunlight reflection by the retroreflector. By adjusting the angle of the retroreflector, the energy hub can redirect the sunlight to those nodes sheltered from trees or other obstacles. The energy hub itself is equipped with a powerful solar panel so that its energy supplement is not the key point of this paper. That is to say, even during the night, energy hubs can provide energy with means of wireless energy transfer. Second, because the sunlight and wireless energy transfer can only generate feeble electric current, we need to find ways to speed and easily store the energy. Regarding the first problem, we need to solve further two more problems. One is how we can find the node and compute the corresponding angle of retroreflector. The other is who and how long we should forward the sunlight to. eLighthouse is suitable for plain area deployment where trees and bush are not too flourishing. The energy hub is often deployed in a relatively open area or higher location and with large energy harvesting equipment so that its own energy consumption needs no considerations. Regarding the second problem, we use super capacitors as the energy storage.

3.2. Hardware Implementation. The architecture of eLighthouse sensor network is shown as in Figure 3, which is composed of two parts, energy harvesting sensor nodes and the equipment called energy hub. The sensor nodes are composed of (i) the sensor board equipped with multiple sensors in which light sensor is a fundamental part while other sensors are optional, (ii) a square 15 cm × 15 cm solar panel for power recharging, (iii) a 10 or 20 F super capacitor for energy storage and supplier, (iv) peripheral circuit for

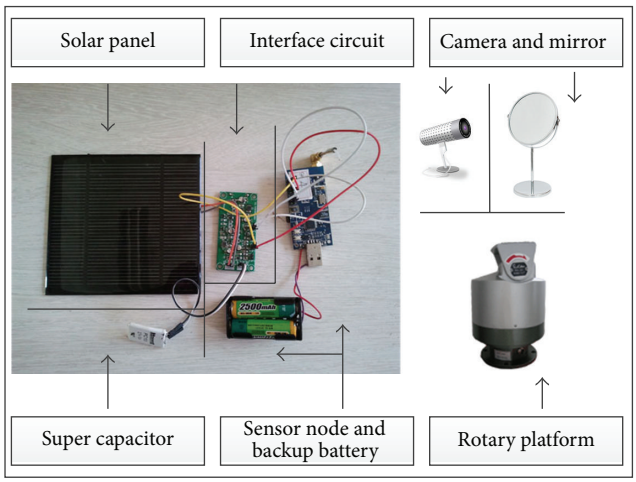

Figure 3: Hardware components of eLighthouse.

energy harvesting and voltage convert; (v) radio transceiver component and a set of backup batteries.

Li-ion or other batteries normally cannot support fast charge and respond slowly to weak charging current. Therefore, using a single Li-ion battery is not enough to satisfy future development of wireless sensor networks. Also the residual energy of Li-ion battery is hard to compute accurately and it does not have a linear relation between residual energy and voltage. Furthermore, for a long-time deployment, charging cycle is essential to the sensor battery. To maximize the usage of energy and schedule sensor nodes efficiently, as well as routing protocol, the residual and charging energy of battery should be accurately calculated. Regarding super capacitor, its residual energy is in accordance with the formula $E = (1/2)CV^2$. Furthermore, super capacitors almost have unlimited charging cycles and can be charged very quickly. In this paper, we design our system using super capacitors as main energy storage and a Li-ion battery as a backup battery. If there is redundant energy, it will be stored in Li-ion batteries. However, energy leakage is a main concern of super capacitors. It means the design of energy using policy, e-hub scheduling, and routing protocols should be carefully addressed against this.

The energy hub consists of (i) a rotary platform that can pan and bend so as to adjust angle of the retroreflector, (ii) a retroreflector which is used to reflect sunlight, and (iii) a camera for accurate localization of node as an assistant of RSSI method. The energy hub is connected to a TelsoB node which will receive residual energy information from other nodes and perform scheduling algorithm to control the rotary platform. In most occasions, the energy hub itself is equipped with a set of powerful energy harvesting devices, for example, with larger area of solar panel. The energy harvested during daylight can be used to charge nodes during the night. However, energy has to be transmitted using wireless means when there is no sunlight. Without losing generality, if we regard energy hubs as all-weather energy suppliers, problems that include how to cover sensor nodes with minimum energy hubs and how to schedule charging sequence will be addressed in Section 5.

3.3. Software Implementation. The software components are built on TinyOS 2.1 and run on each sensor node in the network. Besides normal data collection, the sensor node is running status report task periodically. It also keeps measuring its residual energy status and will require the energy hub to transfer sunlight when the energy is below certain thresholds. The control and scheduling software component is running on the TelosB node attached with the energy hub. It communicates with other nodes through 802.15.4 interface.

Normally, one energy hub provides sunlight transfer to several nodes. We need to identify the following things. First, who shall be responsible for initializing the energy transferring process? Second, how to control sunlight reflection between a pair of sensor node and energy hub? Third, how to balance the collision of multiple energy transferring requirements?

To begin an energy transferring process, there could be two kinds of methods. Namely, energy hub initialized and sensor node initialized schemes. In [11], the node whose energy is going to be below critical level will cast an energy sharing request to nodes listed in descending order of efficiency. However, in a network scale view, energy should be reserved as much as possible. In our design, energy is stored in the super capacitor. Therefore, higher energy reservation will lead to higher energy leakage. Hence, energy pairing is related to two things, energy level and using pattern. When a node's battery is going to be flat, it will be an initializer as in [11]. Also, when in daytime, an energy hub will become an initializer.

If an energy hub and node go into sunlight reflection procedure, the initializer sends out a REFLECTION_REQUEST message. After receiving the message, the other one may answer with message REFLECTION_RESPOND. When a sunlight reflection process starts, the energy hub will generate a REFLECTION_START packet and try to locate the node. The node will direct the locating process with its light sensor. When the desired amount of sun radiation has been transferred, the energy hub sends out the REFLECTION_STOP packet. However, the node can also send out REFLECTION_STOP packet to terminate the sunlight reflection process under certain circumstances.

The software flowchart of sensor nodes is shown in Figure 4. After initiation, sensor nodes always measure their battery level and report to energy hubs. If energy level is below certain threshold, for example, $E_i^{\min}$, the sensor node will send request to ask for energy transferring from the energy hub. Both energy hubs and sensor nodes can initiate energy transfer process so that an energy transfer pairing procedure is brought forward to help balance energy scheduling and emergency battery charging, and so forth. If energy paring is successful, then it will start sunlight reflect process.

The software flowchart of energy hubs is shown in Figure 5. They monitor battery status of appurtenant sensor nodes, analyze their energy consumption and harvesting model, and then perform charging sequence scheduling to

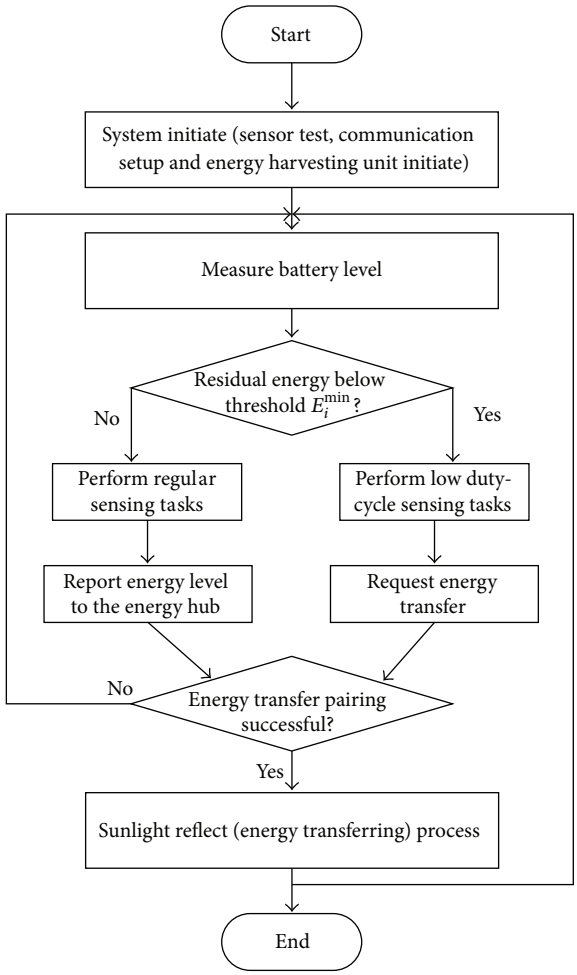

Figure 4: Software flowchart of sensor nodes.

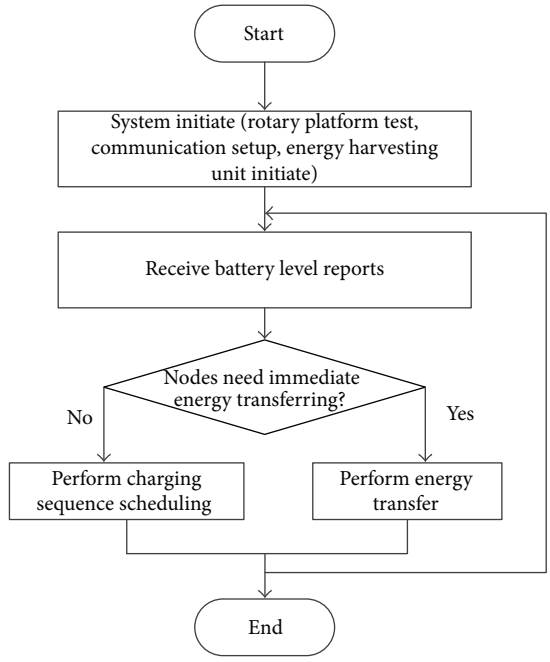

Figure 5: Software flowchart of energy hub.

enable sensor nodes stay working as long as possible. Besides initiating charging in scheduling they need also to respond to immediate energy transfer request.

4. Energy-Aware Node Locating

4.1. Accurate Node Localization. In our proposed scheme, in order to reflect the sunlight accurately to the solar panel of each sensor node, an important step is the localization of all the solar boards. There have been many methods introduced for localization, which are either range-based or range-free [15]. Since range-free approaches use hop count and the average distance as the measurement standard, they are not able to be applied in our scenario which only considers one-hop distance situation.

In our scenario, as the localization precision is relatively high which requires the reflected light directly positioning the solar board, all the above schemes cannot satisfy the requirement. However, the localization in our scenario is not a global network localization; it only covers approximately one-hop distance, or even shorter. A benefit raised from this situation is that we can use video camera on the platform to coordinate the accurate positioning. Light sensor embedded in the sensor node also can help to increase the accuracy by communication feedback. The detailed system procedure, the localization process, and the corresponding geometrical model are shown as follows.

We assume all the sensor nodes are deployed in a plane area, and the height of the retroreflector in the energy hub is known as H. The sink node is connected to the energy hub and located exactly below the retroreflector which is set to be the original point of the coordinate systems. In the sensor node deployment and network initialization stage, the positions of the manually deployed sensor nodes are set to be known parameters. By converting the rectangular coordinate system (x, y, z) to the polar coordinate system (γ, θ, ϕ), the horizontal angle θ and the vertical angle ϕ of the position from the original point to these nodes can be obtained, which will be discussed in the next subsection.

During the long-term monitoring of the sensor network, newly added nodes may change the topology and the connections of the network. Correspondingly, the localization information requires updating. In our method, fundamental RSSI is used as a first step for rough localization. The newly added nodes that will broadcast a short beacon message in a particular transmit power strength, which is power level 10 in CC2420 for our experiment. Those neighborhood nodes that receive this information will use the received signal strength to calculate the distance from the radio source and report it to the sink. The correspondence between distance and the signal strength has been measured in advance. This sink node will select two-distance information from the location-known nodes and that collected by itself to determine the (x, y) location of the new nodes. With the knowledge of D_0, D_1, D_2, (X_1, Y_1), and (X_2, Y_2), it is easy to obtain the value of

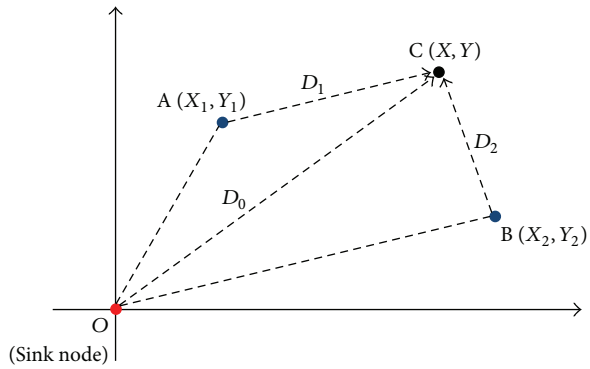

Figure 6: Example of node locating.

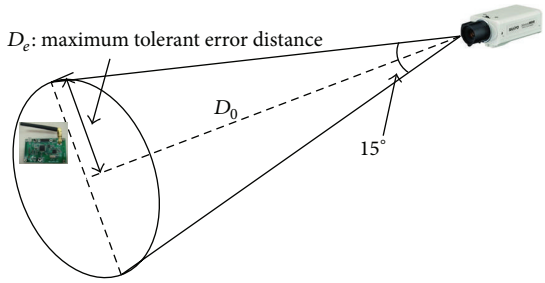

Figure 7: Camera assisted node locating.

(X, Y), which only requires some fundamental geometrical knowledge, as shown in Figure 6.

However, our experiment results show that the error of this RSSI measurement and location calculation is up to a level of 1-2 meters with an approximately 20-meter D_0, which is unacceptable for the application. Therefore, to improve the accuracy of localization, the onboard camera in the rotary platform of energy hub will take the second run. The directional camera used in our experiment has a visual angle of 15°, which is a typical value. In the case of 20-meter D_0, the maximum tolerant error distance for RSSI localization is shown in Figure 7, which is $20 \tan(7.5^\circ) = 2.63$ m, larger than the experiment results. After the camera captured the sensor node solar board, the rotary platform will slightly be rotated until the solar board moves to the center of the camera visual area. Then the exact direction of the solar board can be determined, as shown in Figure 7.

4.2. Single-Node Solar Panel Coverage. It is also a challenge to enable reflected light to fully cover the designated solar panel so that the utility of solar power can be maximized. After accurate node localization, the right angle of retroreflector should be calculated and the hardware component has to be correctly positioned by the rotation of the rotary platform. Then, the minor adjustment will take place to make full coverage according to the response of the sensor node.

Assume that the location of a node has been acquired using our locating algorithm so that we know the distance and height and is able to compute its relative location to the energy hub. The detailed process is described as follows. In Figure 8,

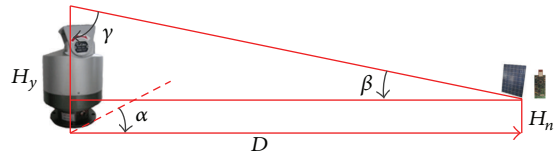

Figure 8: Solar power reflection.

H_n and coordination are known from node localization. H_y is a constant. Hence,

$$\gamma = 90 - \arctan\left(\frac{H_y - H_n}{\sqrt{x^2 + y^2}}\right), \qquad \alpha = \arctan\left(\frac{y}{x}\right). \tag{1}$$

After obtaining γ and α we can control the rotary platform to reach the position.

With the knowledge of the accurate node location, it does not guarantee that the entire surface of the solar panel can be covered by the reflected sunlight. The solar panel may be located to any side of the sensor node, which generates a design challenge of the proposed scheme. In this paper, we use slow moving capturing combined with feedback from the nodes to solve this problem. When the light is reflected to the node, it will result in increasing of luminous flux of light sensor. However, the location related to the solar power has a great impact on performance of the method. We summarize four situations as shown in Figure 9. In Figure 9(a), the light sensor is covered by all the circles while none of the circles provides full coverage of the solar panel. In Figure 9(b), the light sensor is covered by none of the circles while each circle provides full coverage of the solar panel. In Figure 9(c), it is desired situation that the solar panel and the light sensor are both covered. Let us analyze the situation using multiple light sensors. All possible placements of light sensors around the solar panel are shown in Figure 9(d). When two light sensors are deployed separately on the two sides of the solar panel as two yellow dots, in most occasions, we can clarify that the panel is fully covered upon both light sensors being covered. The choices of location are proved as follows.

The placement of light sensors is decided by the size of the solar panel and the light coverage circle. For simplicity, let r stand for the radius of the light circle, let a denote the side length of the solar panel, and let d be the distance between the light sensor and the center of the light panel. Figure 10(a) shows the specified case that two sensor nodes are within maximum distance between each other. The distance d can be calculated as follows:

$$d_1 = \sqrt{r^2 - \left(\sqrt{r^2 - \left(\frac{a}{2}\right)^2} - \frac{a}{2}\right)^2}. \tag{2}$$

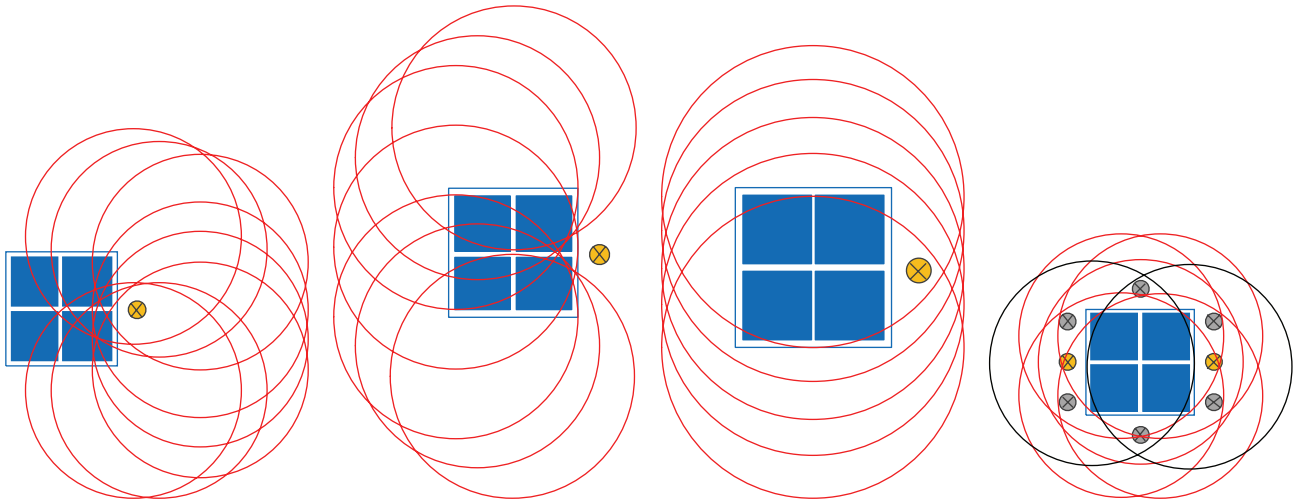

(a) Sensed but not fully covered (b) Fully covered but not sensed (c) Fully covered and sensed (d) Multiple light sensors

FIGURE 9: On single node solar pad coverage.

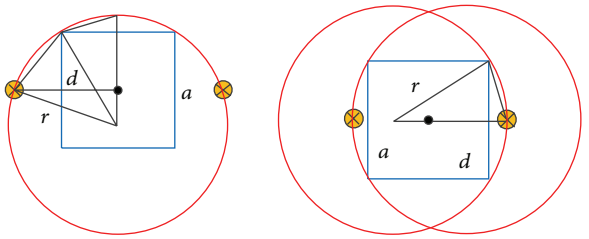

(a) (b)

FIGURE 10: Computing of light sensor placement.

The best placement of light sensor is shown in Figure 10(b), and it can be computed as follows:

$$d_2 = \frac{a}{2} + \left(r - \sqrt{r^2 - \left(\frac{a}{2}\right)^2} \right). \tag{3}$$

As a result, the distance of the light sensor should not be greater than d_1 and is preferred to be d_2.

5. Scheduling of the Charging Sequence

We consider a wireless sensor network $\mathbb{N}$ consisting of N sensor nodes that are randomly distributed in a two-dimensional area of size $X \times Y$. It is assumed that locations of all sensor nodes are known once they are deployed. Each sensor node $n_i, i \in 1, \ldots, N$, is powered by rechargeable battery with maximum capacity $E_i^{\max}$, and a minimum energy level $E_i^{\min}$ is required to keep the node operational. The energy consumption rate of node n_i is assumed to be cr_i. Let $e_i(t)$ be the energy level of node n_i at time t, and we say that a node n_i *stays alive* if $\forall t, e_i(t) \geq E_i^{\min}$.

A number of M energy hubs $\mathbb{H}$ are deployed in the same area to charge the sensor nodes, where each energy hub $H_j, j \in 1, \ldots, M$, is responsible for charging a subset of sensor nodes $\mathbb{N}_j$. We have $\bigcup_{j \in 1,\ldots,M} \mathbb{N}_j = \mathbb{N}$, and $\forall j, k \in 1, \ldots, M, j \neq k, \mathbb{N}_j \bigcap \mathbb{N}_k = \varnothing$. When a sensor node n_i is charged by energy hub H_j, that is, $n_i \in \mathbb{N}_j$, it is said that n_i *is covered by* H_j.

We assume that all energy hubs have unlimited energy capacity, a similar charging power of E^c and effective charging range of R, which means that only nodes within the charging range can be charged by the energy hub. Denote by $\eta_{i,j}$ the charging efficiency of n_i when n_i is charged by H_j, and the efficient charging rate of n_i is then $\eta_{i,j}E^c$. Notice that $\eta_{i,j}$ is affected by several factors. For instance, in wireless charging, $\eta_{i,j}$ is strongly related to $\mathrm{Dist}_{i,j}$, the distance between the node and the energy hub [10], while, using light-reflection charging, $\eta_{i,j}$ does not depend on $\mathrm{Dist}_{i,j}$ that much. In this paper, we assume that $\eta_{i,j}$ can be decided once the locations of node n_i and energy hub H_j are settled. Therefore, for the sake of clarity, we also denote $\eta_{i,j}$ as η_i if n_i is implied to be covered by a nonspecific energy hub. Also notice that $\eta_{i,j} = 0$ if $\mathrm{Dist}_{i,j} > R$.

To keep continuous energy replenishment, each sensor node n_i is charged periodically by its corresponding energy hub H_j. That is, for each charging period T_i^c, n_i is charged by H_j with charging time t_i^c.

The problem that we intend to solve is to find the minimum number of energy hubs, together with their deployment locations and charging sequences of their covered sensor nodes, such that all nodes stay alive.

5.1. System Model. We consider a system consisting of N sensors nodes. Each node n_i has a battery capacity of $E_i^{\max}$ and a minimum energy level $E_i^{\min}$ at which the node is operational.

The energy consumption rate of node n_i is a nonincreasing function $\mathrm{cr}_i(t)$, and we do not restrict it to be linear, as assumed in some related works [9]. Regarding the fact that most sensor nodes perform periodic activities in a certain

scale of time, it is reasonable to assume that $\mathrm{cr}_i(t)$ is a periodic function, that is, $\mathrm{cr}_i(t+k\cdot T_i) = \mathrm{cr}_i(t), \forall k = 1, 2, 3, \ldots$, where T_i is the period of $\mathrm{cr}_i(t)$. Thereby, the total power consumption during T_i is

$$E_i\left(T_i\right) = \int_0^{T_i} \mathrm{cr}_i\left(t\right) dt. \tag{4}$$

The sensor nodes are recharged periodically by the energy hub. Denote E^c the charging power of the charger and η_i the charging efficiency w.r.t. node n_i, and the efficient charging rate for node n_i is then $\eta_i E^c$. Notice that η_i equals zero if node n_i is not chargeable by the energy hub due to reasons like being outside the efficient charging range or being blocked by obstacles. Context switch cost which includes reflector adjustment delay is implied with η_i. Let the length of the recharging time t_i^c be invariable in each period, and the total energy recharged to node n_i during one period T_i is

$$E_i^c\left(T_i\right) = \eta_i E^c t_i^c. \tag{5}$$

Let $e_i(t)$ be the energy level of node n_i at time t, and we say that a node n_i *stays alive* if $\forall t\ e_i(t) \geq E_i^{\min}$. We intend to find that, given the above system, does it exist a feasible schedule such that all nodes stay alive, and if so, how the feasible schedule is generated.

5.2. Problem Description. We first examine some conditions that must be satisfied before the problem is formally defined.

Lemma 1. *A node n_i stays alive if it satisfies*

$$e_i\left(t_{i,k}^0\right) \geq E_i\left(T_i\right) + E_i^{\min}, \quad \forall k = 1, 2, 3, \ldots, \tag{6}$$

where $t_{i,k}^0$ denotes the time instance at the beginning of the kth period.

Proof. We prove the following by contradiction. Assume the node goes dead during the mth period at time $t' \in [t_{i,m}^0, t_{i,m}^0 + T_i]$, and then

$$e_i\left(t'\right) = e_i\left(t_{i,m}^0\right) - E_i\left(t_{i,m}^0, t'\right) + E_i^c\left(t_{i,m}^0, t'\right) < E_i^{\min}, \tag{7}$$

where $E_i(t_1, t_2)$ and $E_i^c(t_1, t_2)$ denote the consumed energy and recharged energy during times t_1 and t_2, respectively. Therefore, we have

$$\begin{aligned} e_i\left(t_{i,m}^0\right) &< E_i^{\min} + E_i\left(t_{i,m}^0, t'\right) - E_i^c\left(t_{i,m}^0, t'\right) \\ &\leq E_i^{\min} + E_i\left(t_{i,m}^0, t'\right) \\ &\leq E_i^{\min} + E_i\left(T_i\right) \end{aligned} \tag{8}$$

which contradicts (6). □

Assume that $e_i^{\mathrm{init}} = e_i(t_{i,1}^0)$ is the energy level at the beginning of the first period; according to Lemma 1, the following condition must be satisfied

$$e_i^{\mathrm{init}} \geq E_i^{\min} + E_i\left(T_i\right). \tag{9}$$

Lemma 2. *A node n_i stays alive only if it satisfies*

$$E_i^c\left(T_i\right) \geq E_i\left(T_i\right). \tag{10}$$

Proof. We prove the following by contradiction. If $E_i^c(T_i) < E_i(T_i)$, then $\exists m$, such that at time $t' \in [t_{i,m}^0, t_{i,m}^0 + T_i]$

$$\begin{aligned} e_i\left(t'\right) &= e_i^{\mathrm{init}} + \sum_{k=1}^{m}\left(E_i^c\left(T_i\right) - E_i\left(T_i\right)\right) \\ &\quad + E_i^c\left(t_{i,m}^0, t'\right) - E_i\left(t_{i,m}^0, t'\right) \\ &< 0 \leq E_i^{\min} \end{aligned} \tag{11}$$

which means the node goes dead at time t', and therefore the lemma follows. □

From Lemma 2 and (5), we deduce that

$$E_i^c\left(T_i\right) = \eta_i E^c t_i^c \geq E_i\left(T_i\right) \tag{12}$$

which gives the recharging time

$$t_i^c \geq \frac{E_i\left(T_i\right)}{\eta_i E^c}. \tag{13}$$

However, it is not sufficient to claim that a node stays alive if the recharging time satisfies (13). This is because if recharging happens when the energy level of node n_i reaches $E_i^{\max}$, the recharging efficiency reduces to the equivalent value of the energy consumption rate at that time (thus keeping the energy level at $E_i^{\max}$). Therefore, the actual recharged energy during that period is less than the designated $E_i^c(T_i)$. On the other hand, such recharging wastes energy and time of the charger and accordingly the opportunity of maintaining other nodes operational. The following lemma prevents such insufficient charging time.

Lemma 3. *A node n_i with charging efficiency $\eta_i E^c$ is guaranteed to be recharged with energy of amount $E_i^c(T_i)$ evaluated as in* (5) *using recharging time t_i^c if*

$$e_i\left(t_{i,k}^0\right) \leq E_i^{\max} - E_i^c\left(T_i\right), \quad \forall k = 1, 2, 3, \ldots. \tag{14}$$

Proof. The node is guaranteed to be recharged with energy of amount $E_i^c(T_i)$ using recharging time t_i^c if and only if during charging the energy level does not exceed $E_i^{\max}$.

We then prove the following by contradiction. Assume the energy level exceeds $E_i^{\max}$ at time $t' \in [t_{i,m}^0, t_{i,m}^0 + T_i]$, and then

$$e_i\left(t'\right) = e_i\left(t_{i,m}^0\right) + E_i^c\left(t_{i,m}^0, t'\right) - E_i\left(t_{i,m}^0, t'\right) > E_i^{\max} \tag{15}$$

which gives

$$\begin{aligned} e_i\left(t_{i,m}^0\right) &> E_i^{\max} - E_i^c\left(t_{i,m}^0, t'\right) + E_i\left(t_{i,m}^0, t'\right) \\ &\geq E_i^{\max} - E_i^c\left(T_i\right) \end{aligned} \tag{16}$$

which contradicts (14). □

Lemma 4. *A node n_i with charging efficiency $\eta_i E^c$ is guaranteed to be recharged with energy of amount $E_i^c(T_i)$ evaluated as in* (5) *using recharging time t_i^c if*

$$E_i^c\left(T_i\right) = E_i\left(T_i\right). \tag{17}$$

Proof. Regarding (10), if $E_i^c(T_i) > E_i(T_i)$, we have $e_i(t_{i,k+1}^0) = e_i(t_{i,k}^0) + E_i^c(T_i) - E_i(T_i) > e_i(t_{i,k}^0)$, $\forall k$, which means that the energy level at the beginning of each period keeps increasing. Therefore, it is clear that $\exists m$, such that

$$e_i\left(t_{i,m}^0\right) + E_i^c\left(T_i\right) > E_i^{\max} \tag{18}$$

which violates (14) Lemma 3. By contradiction, the lemma follows. □

Equation (17) means that during each period T_i, the consumed energy is equivalent to the recharged energy, and hence the energy level at the beginning of each period remains the same; that is,

$$e_i\left(t_{i,k}^0\right) = e_i^{\text{init}} \quad \forall k. \tag{19}$$

We now formally define the schedulability problem mentioned at the end of Section 5.1.

Definition 5. The system described in Section 5.1, subjected to the following constraints: $\forall i \in N$

$$e_i^{\text{init}} \geq E_i^{\min} + E_i\left(T_i\right), \tag{20}$$

$$e_i^{\text{init}} \leq E_i^{\max} - E_i^c\left(T_i\right), \tag{21}$$

$$t_i^c = \frac{E_i\left(T_i\right)}{\eta_i E^c} \tag{22}$$

stays alive if each node n_i receives t_i^c recharging time in each period T_i.

Notice that (22) can be directly derived from (5) and (17).

5.3. Schedulability Analysis. To guarantee that each node n_i receives t_i^c recharging time during each T_i, it suffices to consider the equivalent problem of tasks scheduling on a uniprocessor, which is described as follows.

Definition 6. The system described in Definition 5 stays alive if and only if N tasks, each of which has period T_i, constant execution time t_i^c, and relative deadline $D_i = T_i$, are schedulable on a uniprocessor.

Using the well-established scheduling theory of real-time systems [26], we have the following.

Lemma 7. *The system described in Definition 5 stays alive if*

$$\sum_{i=1}^{N} \frac{t_i^c}{T_i} \leq B, \tag{23}$$

where B depends on different scheduling algorithms and equals 1 or $N(2^{1/N}-1)$ if earliest deadline first (EDF) or rate monotonic (RM) algorithm is used [27], respectively. Notice that, using EDF, the condition of (23) *is necessary and sufficient, while, using RM, it is only sufficient condition. For interested readers, please refer to [26] for details.*

Equation (23) shows that smaller recharging time t_i^c helps improve the schedulability of the system. With respect to (10), this argument strengthens (17).

5.4. Selection of e_i^{init}. From (20) and (21), we know that e_i^{init} must be set in the range of $[E_i^{\min} + E_i(T_i), E_i^{\max} - E_i^c(T_i)]$. It is worth mentioning that the schedulability condition of (23) is not affected by the timing when e_i^{init} is reached. This means whenever the energy level of node n_i reaches the decided value e_i^{init}, it immediately joins the charging scheduling and starts its first period.

Also notice that keeping e_i^{init} at a not-too-high level also helps reducing the leakage of the battery. As shown in [4], ultracapacitors lose electrical energy even when there is no operation, and the problem of leakage is more serious when the energy level is high. Therefore, keeping the energy level at a moderate level benefits the reservation of battery power.

5.5. Selection of the Period T_i. In this section, we discuss the selection of the period T_i for a node n_i. We select T_i according to the periodicity of the node's activities. However, a node may repeat its activities with high frequency, resulting in a short period. This may lead to a nonnegligible "context switch" cost if preemptive scheduling is applied. Therefore, in practice, T_i could be set multiple times the actual period of the repetitive activities of node n_i.

On the other hand, from (17), (20), and (21), we have

$$E_i^{\min} + E_i\left(T_i\right) \leq e^{\text{init}} \leq E_i^{\max} - E_i\left(T_i\right) \tag{24}$$

resulting in

$$E_i\left(T_i\right) \leq \frac{E_i^{\max} - E_i^{\min}}{2} \tag{25}$$

which puts a constraint on the maximum value of T_i.

Meanwhile, certain energy-harvesting methods, for example, solar power, pose a limitation on the available charging time. Furthermore, when the characteristics of the power source or node workload (and accordingly the power consumption) change, the schedule must adapt to the variation. It would then not be suitable to choose a too long period in such circumstance.

In a word, period T_i should be wisely selected, making balance between several factors.

5.6. Energy Hub Coverage. As described in [28], the problem of covering all sensor nodes using a number of charger nodes is not similar to the widely studied coverage problem in Wireless Sensor Networks. The latter one can be mainly of two types: area coverage and target/point coverage, which intend to find the required number and exact locations of sensor nodes that cover an entire piece of area or a limited number of targets. While our problem, on the other hand, is to find a minimum number of energy hubs and their corresponding locations such that all sensor nodes in the network will receive continuous energy replenishment.

We adopt the framework proposed in [28], which utilized grid approximation, minimum set cover problem, and greedy

```
function LOCATE_CHARGERS(X, Y, s, R, ℕ)
    ℕ_uncovered ← ℕ, ℍ ← ∅
    while ℕ_uncovered not equal ∅
        H_j, ℕ_j ← LOCATE_NEXT(X, Y, s, R, ℕ_uncovered)
        if ℕ_j equals ∅
            exit "Not feasible"
        end if
        ℕ_uncovered ← ℕ_uncovered − ℕ_j
        ℍ ← ℍ + {H_j}
    end while
    return ℍ
end function
```

Pseudocode 1: Pseudocode of the algorithm for finding the locations of energy-hubs to cover all sensor nodes.

approach. The difference lies in the fact that we do not neglect the charging time and consider real-time charging scheme, while in, [28], the charging time is assumed negligible and an energy hub is able to charge all sensor nodes within a certain range. Thereby, in our algorithm, sensor nodes that will be covered by an energy hub must satisfy that (1) they are within the energy hub's effective charging range R and (2) they do not violate (23).

To convert the infinite search space to finite one, the grid approximation technique is applied, where the deployment area of sensor nodes with size $X \times Y$ is divided into grids with size $s \times s$, and all energy hubs will only be placed on the grid points. At the cost of losing optimality, this conversion significantly reduces complexity and saves computation time of the algorithm.

Energy hubs are located one by one. At each step, the best location of an energy hub is obtained by testing in the finite search space. Upon finding the best location for the energy hub, its covered sensor nodes are removed. The next energy hub is to be found in the same manner but considering only sensor nodes that have not yet been covered by any energy hub. The procedure continues until all sensor nodes are covered. The pseudocode is shown in Pseudocode 1.

It is shown that at each step of the while loop, a function **LOCATE_NEXT** is invoked to return the next energy hub H_j and its covered sensor nodes $\mathbb{N}_j$. Pseudocode 1 also shows an interesting point that if, at any step, an energy hub is not able to cover any sensor node, it can be concluded that there is no feasible solution to the problem. In that case, a smaller grid size s is desirable. In fact, a smaller value of s, though making the search more time consuming, usually leads to a closer solution to the optimal one, because it gives a finer approximation of the infinity search space.

Each step of finding the location of the next energy hub H_j, accomplished by function **LOCATE_NEXT**, is proceeded in a greedy way. That means we search every grid point and pick the one on which, if an energy hub is deployed, the maximum number of sensor nodes will be covered. In particular, from each grid point (x, y), the energy hub H_j is assumed to be placed to check how many sensor nodes it is able to cover. This is achieved by calculating the distance $\text{Dist}_{i,j}$ between each sensor node n_i, located at (x_i, y_i), and this grid point, and then comparing it with the charging range R. It is assumed that the location of each sensor node is known using GPS or other localization methods [29]. To guarantee the condition given by Lemma 7, only a subset of all the sensor nodes that are within the charging range R and do not violate (23) will be selected as the nodes covered by the energy hub. For each such placement of energy hub on a grid point, we pick the one where the maximum number of sensor nodes will be covered, denoting the ratio between t_i^c and T_i^c as U_i. If there are several such grid points giving the same maximum number, we select the one where a smaller sum of U_i is achieved. The pseudocode is shown in Pseudocode 2.

Notice that, in the pseudocode shown in Pseudocode 2 at each grid point (x, y), the set of sensor nodes that are within the charging range R, denoted by $\mathbb{N}_j'$, are ordered with respect to U_i in nonincreasing order, and the first several nodes that lead to violation of (23) will be removed from the set. This is to make sure that a larger number of nodes will be selected to be covered. On the other hand, nodes with smaller U_i are preferable due to the fact that smaller U_i implies better charging efficiency.

6. Evaluation and Experiments

We both use simulation and testbed to evaluate our proposed methods.

6.1. eHub Coverage. This section will demonstrate the effectiveness and performance of the proposed algorithm. In addition, the method presented in [28] will also be tested and compared with our algorithm. In particular, we denote the two methods as follows.

(i) *Greedy-R-based* refers to the method proposed in [28] where, at each step of locating the next charger, the greedy search selects the grid point where maximum number of sensor nodes will be covered based on the criterion that they are within the charging range R.

(ii) *Greedy-U-based* is the method presented in this paper and differs from the above method in the criterion of determining which sensor nodes will be covered, where the condition of (23) must be also considered.

```
function LOCATE_NEXT (X, Y, s, R, ℕ_uncovered)
  #nodes_covered ← 0, U ← 0, H_j ← ∅, ℕ_j ← ∅
  for x = 0 to X step s
    for y = 0 to Y step s
      H'_j ← (x, y)
      ℕ'_j ← ∅
      for each n_i ∈ ℕ_uncovered
        if Dist_{i,j} <= R
          ℕ'_j ← ℕ'_j + {n_i}
        end if
      end for each
      order ℕ'_j w.r.t. U_i in non-increasing order
      for each n_i ∈ ℕ'_j
        if Σ_{n_k ∈ ℕ'_j} U_k > B
          ℕ'_j ← ℕ'_j − {n_i}
        end if
      end for each
      U' = Σ_{n_i ∈ ℕ'_j} U_i
      if |ℕ'_j| > #nodes_covered or
      (|ℕ'_j| equals #nodes_covered and U' < U)
        #nodes_covered ← |ℕ'_j|
        U ← U'
        H_j ← H'_j
        ℕ_j ← ℕ'_j
      end if
    end for
  end for
  return H_j, ℕ_j
end function
```

Pseudocode 2: Pseudocode of the function to find the next energy-hub.

In the first simulation, we randomly deploy 12 sensor nodes in an area with dimension of 50 m × 50 m. The grid approximation of this area uses a step size of $s = 5$ m. Each node's battery has the same $E^{\max} = 10$ J and $E^{\min} = 0$ J. (In practice, $E^{\min}$ is required to be slightly above 0 for a sensor node to be operational. However, $E^{\min} = 0$ will not jeopardize the correctness of our simulation results, but improves readability.) For each node n_i, the charging period T_i^c is given the value randomly distributed in the range $[50, 100] \times 10^3$ sec, the energy consumption rate cr_i is evaluated as $E^{\max}/2/T_i$, and the initial energy level equals $E^{\max}/2$, which are set in accordance with (6) and (14).

For each energy hub to be deployed, it has charging power $E^c = 10.0$ W and charging range $R = 10.5$ m. The charging efficiency $\eta_{i,j}$ of each node depends on its distance to the energy hub H_j and is obtained using the following equation:

$$\eta_{i,j} = 1.1522^{-\mathrm{Dist}_{i,j}-21.1498}. \quad (26)$$

The function of $\eta_{i,j}$ is built from experience and implies that $\eta_{i,j}$ decreases as $\mathrm{Dist}_{i,j}$ increases and reaches 1.5% when $\mathrm{Dist}_{i,j} = R$. In addition, the maximum value of $\eta_{i,j}$ is assumed to be 5%.

The simulation is performed in Matlab, and its results of finding deployment of energy hubs using *Greedy-R-based* method and *Greedy-U-based* method, respectively, are shown in Figure 11. In the figures, dashed lines mark the grid, small solid squares denote sensor nodes, and each circle denotes an energy hub's charging range, while an energy hub is located at the center of a circle that coincides with a grid point. The location of each energy hub is labeled as H_i, where the suffix i is in accordance with the ordering given by the greedy search procedure.

It is shown in Figure 11(a) that, using *Greedy-R-based* method, the first energy hub H_1 is put on the grid point of $(10, 15)$, covering 4 sensor nodes. The second energy hub H_2 is put at $(10, 40)$ and also covers 4 sensor nodes. The 3rd and 4th energy hubs then cover 3 and 1 sensor nodes, respectively. Differently, the *Greedy-U-based* method generates the deployment, shown in Figure 11(b), where H_1 is located at $(10, 10)$, covering 3 nodes, H_2 is put at $(5, 40)$, covering 3 nodes, H_3 covers 3 nodes, and H_4 covers 2 nodes, while an extra H_5 covers the last node.

The difference of the results produced by two methods is due to the fact that, when charging time is non-negligible, an energy hub is only capable of charging a limited number of its neighboring sensor nodes. To clarify our point, we have

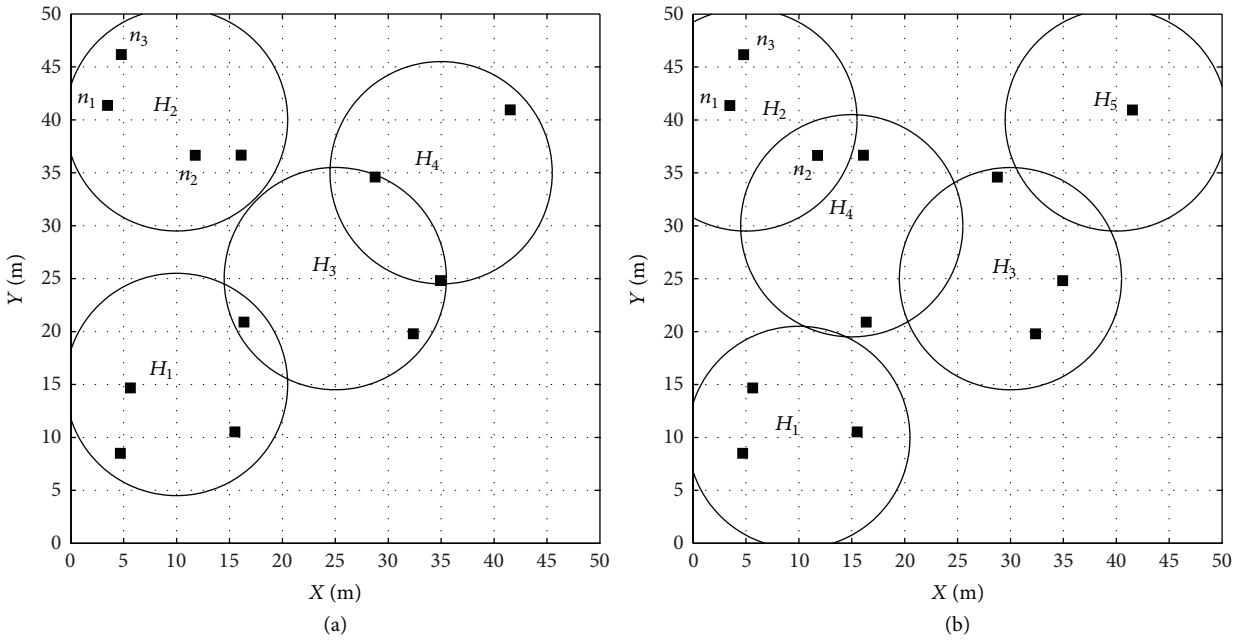

Figure 11: Deployment of energy hubs using *Greedy-R-based* and *Greedy-U-based* methods.

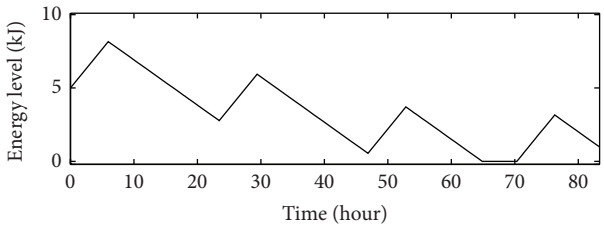

Figure 12: Energy level of node n_1 using *Greedy-R-based* and FIFO scheduling.

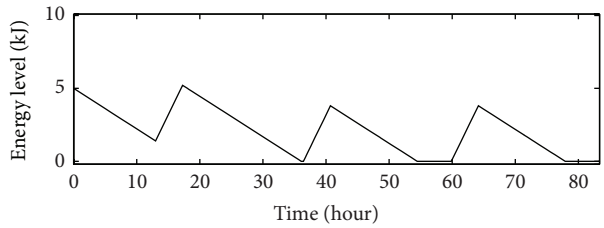

Figure 13: Energy level of node n_2 using *Greedy-R-based* and EDF scheduling.

performed another simulation of charging the 4 sensor nodes covered by energy hub H_2 in Figure 11(a). The simulation is written with TrueTime [30], a real-time scheduling toolbox in Matlab, and is simulated for 3×10^6 seconds.

Figure 12 shows the energy level of node n_1, located at (3.47, 41.37), when the energy hub schedules the charging sequence of its 4 covered sensor nodes in FIFO order. It is shown that around 65 hours, the battery of the sensor node is depleted and its energy level reaches 0.

Furthermore, even when a real-time scheduling algorithm is applied for the charging sequence scheduling, it is still not able to guarantee that all sensor nodes stay alive. In Figure 13, we show the energy level of node n_2, located at (11.77, 36.65), when the energy hub schedules the charging sequence using EDF algorithm [27]. It clearly shows that the energy of n_2 is exhausted around 54 hours.

In contrast, the deployment of energy hubs obtained by our proposed method (*Greedy-U-based*) guarantees the required charging time of each sensor node and manages to keep the energy level of all sensor nodes above $E^{\min}$. In Figure 14, energy levels of the 3 sensor nodes that are covered by energy hub H_2 have been plotted. The figure shows that,

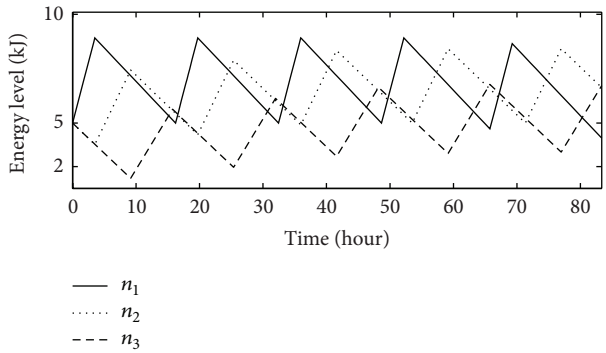

Figure 14: Energy levels of the 3 sensor nodes covered by energy hub H_2 using *Greedy-U-based* and EDF scheduling.

using *Greedy-U-based* method for deploying the energy hubs and EDF algorithm for scheduling the charging sequence, no sensor node's energy level drops below zero during the simulation. Due to the limited space, energy levels of the rest sensor nodes will not be shown in this paper.

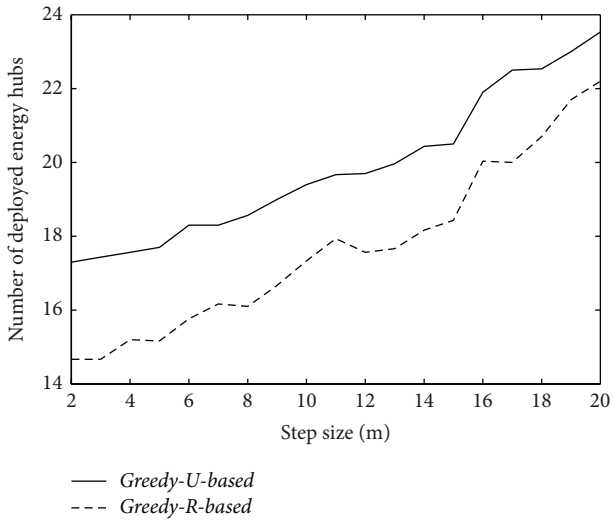

Figure 15: Comparison of the number of deployed energy hubs w.r.t. the step size of grid approximation.

To evaluate the performance of the proposed algorithm, the third simulation is performed. In this simulation, 80 sensor nodes are randomly deployed in a 100 m × 100 m area. Each energy hub has charging power $E^c = 20.0$ W and charging range $R = 15$ m. The rest of the parameter settings are the same as in the first simulation. We vary the step size s of the grid approximation from 2 m to 20 m. For each s, the locations and charging periods of the 80 sensor nodes are randomly generated for 30 times. For each random generation of sensor nodes, we perform both *Greedy-R-based* and *Greedy-U-based* methods and record the number of deployed energy hubs, respectively. The result is summed up and averaged by 30 for each s, which is then plotted in Figure 15.

Figure 15 shows that a smaller step size of grid approximation leads to a smaller number of required energy hubs, for both methods. On the other hand, the number of deployed energy hubs acquired by *Greedy-U-based* method is larger than that by *Greedy-R-based* method. This is true because *Greedy-U-based* method considers not only the charging range R but also the schedulability of an energy hub's covered sensor nodes and hence requires more energy hubs to cover all sensor nodes. Notice that the gap between two methods is not significant with respect to the number of sensor nodes and decreases as step size enlarges.

6.2. Charging Scheduling. Two simulations have been conducted to verify the effectiveness of the scheduling policy described in Section 5.

In the first simulation, we consider a system with 3 sensor nodes, each powered by a super capacitor with the maximum voltage level $E_i^{\max} = 2.5$ V, while its minimum voltage level is assumed to be 0. Every T_i' time, each sensor node performs a specific activity (sampling, transmission, etc.) that takes C_i time and consumes energy at consumption rate cr_i. Taking into account the constraint of (25), we let the charging period T_i for each node be N_i times T_i'.

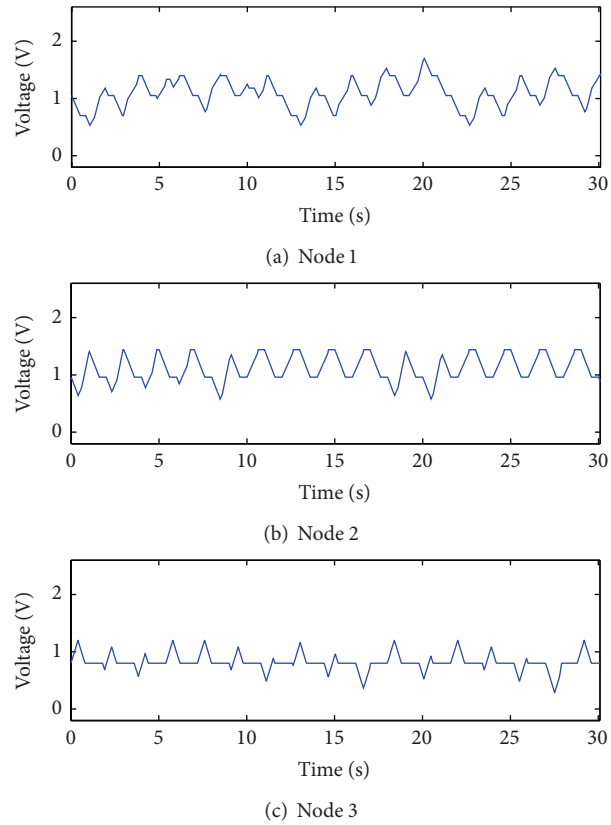

Figure 16: Recharging three sensor nodes using EDF scheduling algorithm.

Table 1 listed the setting is of the above parameters, as well as the resulting $E_i(T_i)$ and the setting of the efficient charging rates $\eta_i E^c$ and charging time t_i^c. Notice that the efficient charging rates are set different to reflect the different lengths between sensor nodes and the energy hub.

Using EDF as the scheduling algorithm, we have

$$\sum_{i=1}^{3} \frac{t_i^c}{T_i} = 0.9068 \leq 1 \tag{27}$$

which guarantees that all three sensor nodes will be recharged in time and kept operational.

Let $e^{\mathrm{init}} = E_i(T_i)$ for each node; the simulation is run for 30 sec using Matlab and TrueTime [31], and the result is shown in Figure 16. It shows that, using EDF real-time scheduling algorithm, all three sensor nodes managed to keep their energy level between $E^{\min}$ and $E^{\max}$ and stay alive.

6.3. Evaluation on Real Platform. We also build a proof-of-concept system to evaluate proposed model. The experiments are established on real solar-powered sensor network. Our experiment can be categorized into two parts. First, we conduct tests on how different ranges of reflection affect the sensor node with solar power harvesting component. This is to evaluate the possibility of transfer energy by

Table 1: Parameters of sensor nodes.

Nodes	T_i'	C_i	cr_i	N_i	T_i	$E_i(T_i)$	$\eta_i E^c$	t_i^c
1	0.8	0.5	0.7	3	2.4	1.05	1.2	0.875
2	1	0.6	0.8	2	2	0.96	1.5	0.64
3	1.8	0.8	1	1	1.8	0.8	2	0.4

T_i', C_i, T_i, t_i^c are in sec; cr_i, $\eta_i E^c$ are in V/sec; $E_i(T_i)$ is in V

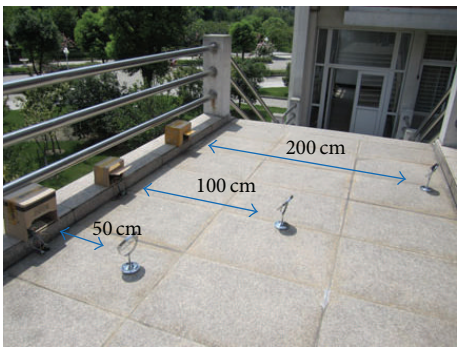

Figure 17: Experiment of three different reflection distance.

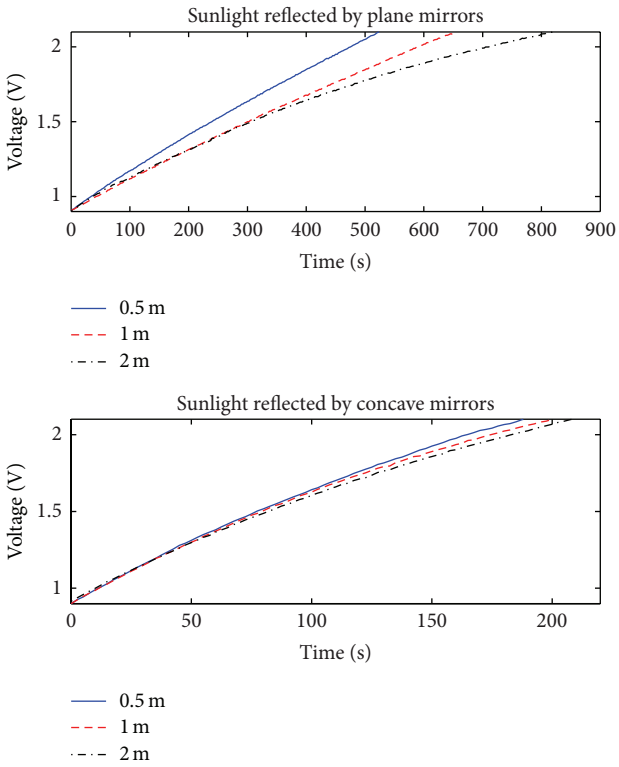

Figure 18: Charging facts with different mirror type and distance.

reflecting sunlight and its efficiency. Furthermore, we obtain charging pattern when distance and luminous intensity vary in different scenario. Second, we use a flashlight as simulated sun light and form a real network to examine node locating algorithm and performance of scheduling.

As seen in Figure 17, we sets up three set of sun light reflection systems which are 50 cm, 100 cm, and 200 cm, respectively. The experiments are conducted using plane mirrors and concave mirrors, respectively. From Figure 18 we can know that using concave will get better efficiency. It will only take 3 minutes to charge the super capacitor while plane mirrors need about 10 minutes to achieve the same goal. No matter what kind of methods are used, the charging efficiency is better than that of magnetic resonance. As expected, the distance between energy hub and receiver will affect the efficiency. Energy experience loss due to scattering while range increases. However, it is hard to tell the difference between three distances when concave mirrors are employed.

We also evaluated our model in an environmental deployment as shown in Figure 19. Node 2 is directly facing the sun and others are in the shadow of trees. Each node will report its status periodically. If their energy drops to a certain degree, they will ask for energy transfer. Then, the energy hub will turn to transfer energy simulated as in the light of the flashlight. If more than one node is in shadow, the energy hub will turn to the one which has higher priority computed using scheduling algorithm. If a new node is added, the energy hub will locate it by RSSI. After that a test reflection will be conducted to measure the exact location. Then, the coordination of the new node will be recorded by the energy hub.

To evaluate node allocating and functionality of scheduling algorithm we performed indoor experiments as shown in Figure 20. We set up an energy hub with eight stationary nodes and use flashlight to simulate reflected sunlight. Each node will report its status periodically. When a node is shaded it will ask for energy transfer. We use boxes to shade one node at a time. The energy hub will turn to and direct the flashlight to the node to simulate the energy transferring procedure. If multiple nodes are in shadow, the energy hub will turn to the one which has higher priority computed using scheduling algorithm. We also did experiment of adding a new node. When a new node is deployed, the energy hub will locate it by RSSI and camera. After that, a test reflection will be conducted to measure the exact location. The charging efficiency of flashlight is shown in Figure 21. The experiments show that the proposed model is feasible.

7. Conclusion

This paper has presented an energy share system to coordinate the energy harvesting wireless sensor network to achieve

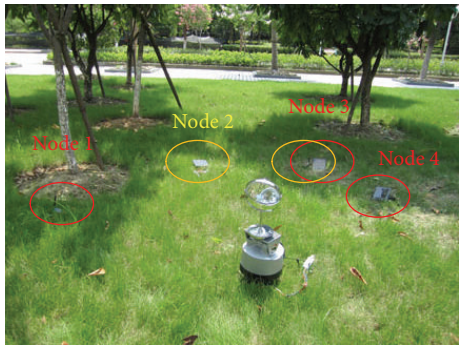

Figure 19: Outdoor deployment of the eLighthouse system.

Figure 20: Indoor testbed using flashlight.

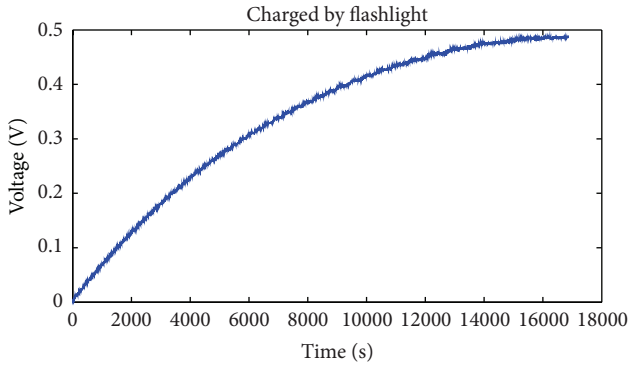

Figure 21: Charging facts of flashlight.

energy balance and lifetime prolonging. It has clarified that, by using solar power reflection system, efficient initial state energy transfer can be achieved with inexpensive energy hub equipment. A simple but effective scheme for short distance sensor node accurate localization has been introduced and demonstrated as well as the sunlight retroreflector positioning method. The practical experiments prove the correctness of the design criteria and provide an outstanding performance. An introduction of the energy-aware scheduling mechanism has been carried out along with the derivation of the accuracy, which enables the network to be energy balanced and sustainable. Through the proposed approach and corresponding algorithm, a novel way of achieving lifetime maintenance and energy balance in Wireless Sensor Networks has been pointed out with high potential.

eLighthouse system has its own limitation during night or unfavorable weather. In the future, we plan to extend the work by considering cooperative charge, in the sense that a sensor node can be charged by more than one energy hub. In fact, we have assumed in this paper that energy hubs have unlimited energy. Although this is a reasonable assumption when energy hubs are located in environment where the energy for harvesting is abundant, this may not hold in certain practical scenarios. In that case, assigning a set of sensor nodes to only one energy hub for charging is not sufficient, and a multiple coverage scheme is required to handle this issue.

Acknowledgments

This work is supported by the National Natural Science Foundation of China (Grant no. 60903167, 61202093, and 61272539), the Zhejiang Province Natural Science Foundation (Grant no. Y1110831), the subfoundation of Zhejiang Provincial Key Innovation Team on Sensor Networks under Grant no. 2009R50046-4, and the Scientific Research Foundation for the Returned Overseas Chinese Scholars, State Education Ministry.

References

[1] F. Ye, G. Zhong, J. Cheng, S. Lu, and L. Zhang, "PEAS: a robust energy conserving protocol for long-lived sensor networks," in *Proceedings of the 23th IEEE International Conference on Distributed Computing Systems*, pp. 28–37, May 2003.

[2] T. Van Dam and K. Langendoen, "An adaptive energy-efficient MAC protocol for wireless sensor networks," in *Proceedings of the 1st International Conference on Embedded Networked Sensor Systems (SenSys '03)*, pp. 171–180, November 2003.

[3] M. Cardei and D.-Z. Du, "Improving wireless sensor network lifetime through power aware organization," *Wireless Networks*, vol. 11, no. 3, pp. 333–340, 2005.

[4] J. Qiu, B. Lin, P. Liu, S. Zhang, and G. Dai, "Energy level based transmission power control scheme for energy harvesting WSNs," in *Proceedings of the 54th Annual IEEE Global Telecommunications Conference: "Energizing Global Communications" (GLOBECOM '11)*, pp. 1–6, Houston, Tex, USA, December 2011.

[5] G. W. Challen, J. Waterman, and M. Welsh, "IDEA: integrated distributed energy awareness for wireless sensor networks," in *Proceedings of the 8th Annual International Conference on Mobile Systems, Applications and Services (MobiSys '10)*, pp. 35–48, ACM, June 2010.

[6] J. Yun, S. Patel, M. Reynolds, and G. Abowd, "A quantitative investigation of inertial power harvesting for human-powered devices," in *Proceedings of the 10th International Conference on Ubiquitous Computing (UbiComp '08)*, pp. 74–83, ACM, September 2008.

[7] J. Taneja, J. Jeong, and D. Culler, "Design, modeling and capacity planning for micro-solar power sensor networks," in *Proceedings of the International Conference on Information Processing in Sensor Networks (IPSN '08)*, pp. 407–418, St. Louis, Mo, USA, April 2008.

[8] A. Kurs, A. Karalis, R. Moffatt, J. D. Joannopoulos, P. Fisher, and M. Soljačić, "Wireless power transfer via strongly coupled magnetic resonances," *Science*, vol. 317, no. 5834, pp. 83–86, 2007.

[9] Y. Shi, L. Xie, Y. T. Hou, and H. D. Sherali, "On renewable sensor networks with wireless energy transfer," in *Proceedings of the IEEE (INFOCOM '11)*, pp. 1350–1358, Shanghai, China, April 2011.

[10] Y. Peng, Z. Li, W. Zhang, and D. Qiao, "Prolonging sensor network lifetime throughwireless charging," in *Proceedings of the 31st IEEE Real-Time Systems Symposium (RTSS '10)*, pp. 129–139, San Diego, Calif, USA, December 2010.

[11] T. Zhu, Y. Gu, T. He, and Z.-L. Zhang, "EShare: a capacitor-driven energy storage and sharing network for long-term operation," in *Proceedings of the 8th ACM International Conference on Embedded Networked Sensor Systems (SenSys '10)*, pp. 239–252, ACM, November 2010.

[12] A. Savvides, C.-C. Han, and M. B. Strivastava, "Dynamic fine-grained localization in ad-hoc networks of sensors," in *Proceedings of the 7th Annual International Conference on Mobile Computing and Networking*, pp. 166–179, July 2001.

[13] D. Niculescu and B. Nath, "Ad hoc positioning system (APS) using AOA," in *Proceedings of the 22nd Annual Joint Conference on the IEEE Computer and Communications Societies*, pp. 1734–1743, April 2003.

[14] P. Bahl and V. N. Padmanabhan, "RADAR: an in-building RF-based user location and tracking system," in *Proceedings of the 19th Annual Joint Conference of the IEEE Computer and Communications Societies (INFOCOM '00)*, pp. 775–784, March 2000.

[15] Z. Zhong and T. He, "Achieving range-free localization beyond connectivity," in *Proceedings of the 7th ACM Conference on Embedded Networked Sensor Systems (SenSys '09)*, pp. 281–294, ACM, November 2009.

[16] S. Rallapalli, L. Qiu, Y. Zhang, and Y.-C. Chen, "Exploiting temporal stability and low-rank structure for localization in mobile networks," in *Proceedings of the 16th Annual Conference on Mobile Computing and Networking (MobiCom '10)*, pp. 161–172, ACM, September 2010.

[17] W. Xi, Y. He, Y. Liu et al., "Locating sensors in the wild: pursuit of ranging quality," in *Proceedings of the 8th ACM International Conference on Embedded Networked Sensor Systems (SenSys '10)*, pp. 295–308, November 2010.

[18] M. I. Afzal, W. Mahmood, S. M. Sajid, and S. Seoyong, "Optical wireless communication and recharging mechanism of wireless sensor network by using ccrs," *International Journal of Advanced Science and Technology*, vol. 13, no. 1, pp. 49–69, 2009.

[19] A. A. Syed, Y. Cho, and J. Heidemann, "Demo abstract: energy transference for sensornets," in *Proceedings of the 8th ACM International Conference on Embedded Networked Sensor Systems (SenSys '10)*, pp. 397–398, November 2010.

[20] R. Doost, K. R. Chowdhury, and M. Di Felice, "Routing and link layer protocol design for sensor networks with wireless energy transfer," in *Proceedings of the 53rd IEEE Global Communications Conference (GLOBECOM '10)*, pp. 1–5, Miami, Fla, USA, December 2010.

[21] K. Li, H. Luan, and C.-C. Shen, "Qi-ferry: energy-constrained wireless charging in wireless sensor networks," in *Proceedings of the Wireless Communications and Networking Conference (WCNC '12)*, pp. 2515–2520, 2012.

[22] L. Xie, Y. Shi, Y. T. Hou, and H. D. Sherali, "Making sensor networks immortal: an energy-renewal approach with wireless power transfer," *IEEE/ACM Transactions on Networking*, vol. 20, no. 6, pp. 1748–1761, 2012.

[23] C. M. Angelopoulos, S. Nikoletseas, T. P. Raptis, C. Raptopoulos, and F. Vasilakis, "Efficient energy management in wireless rechargeable sensor networks," in *Proceedings of the 15th ACM International Conference on Modeling, Analysis and Simulation of Wireless and Mobile Systems (ACM '12)*, pp. 309–316.

[24] M. K. Watfa, H. AlHassanieh, and S. Selman, "Multi-hop wireless energy transfer in WSNs," *IEEE Communications Letters*, vol. 15, no. 12, pp. 1275–1277, 2011.

[25] M. Erol-Kantarci and H. T. Mouftah, "Mission-aware placement of rfbased power transmitters in wireless sensor networks," in *Proceedings of the IEEE Symposium on Computers and Communications (ISCC '12)*, pp. 000012–000017, Cappadocia, Turkey, 2012.

[26] G. C. Buttazzo, *Hard Real-Time Computing Systems: Predictable Scheduling Algorithms and Applications*, Springer, New York, NY, USA, 2nd edition, 2004.

[27] C. L. Liu and J. Layland, "Scheduling algorithms for multiprogramming in a hard real-time environment," *Journal of the ACM*, vol. 20, no. 1, pp. 46–61, 1973.

[28] F. T. Jaigirdar, M. M. Islam, and S. R. Huq, "Grid approximation based inductive charger deployment technique in wireless sensor networks," *International Journal of Advanced Computer Science and Applications*, vol. 2, no. 1, pp. 30–37, 2011.

[29] T. He, C. Huang, B. M. Blum, J. A. Stankovic, and T. F. Abdelzaher, "Range-free localization and its impact on large scale sensor networks," *ACM Transactions in Embedded Computing Systems*, vol. 4, pp. 877–906, 2005.

[30] D. Henriksson, A. Cervin, M. Andersson, and K. E. Årzén, "TrueTime: simulation of networked computer control systems," in *Proceedings of the 2nd IFAC Conference on Analysis and Design of Hybrid Systems*, Alghero, Italy, June 2006.

[31] A. Cervin, D. Henriksson, B. Lincoln, J. Eker, and K.-E. Årzén, "How does control timing affect performance?" *IEEE Control Systems Magazine*, vol. 23, no. 3, pp. 16–30, 2003.